IEEE Access
Multidisciplinary | Rapid Review | Open Access Journal

Received 30 November 2022, accepted 10 December 2022, date of publication 19 December 2022,
date of current version 29 December 2022.

Digital Object Identifier 10.1109/ACCESS.2022.3230836

RESEARCH ARTICLE

Interference Mitigation for Non-Overlapping Sub-Band Full Duplex for 5G-Advanced Wireless Networks

XIANGHUI HAN[1,2,3], RUIQI LIU[2,3], (Member, IEEE), XING LIU[2], CHUNLI LIANG[2], XINGGUANG WEI[2], YUPENG HAO[2], ZHAOTAO ZHANG[4], AND SHI JIN[1], (Senior Member, IEEE)

[1]National Mobile Communications Research Laboratory, Southeast University, Nanjing 210096, China
[2]Wireless Research Institute, ZTE Corporation, Xi'an 710114, China
[3]State Key Laboratory of Mobile Network and Mobile Multimedia Technology, Shenzhen 518055, China
[4]Nanjing Research and Development Center of Broadband Wireless Communications, Chinese Academy of Sciences (CAS), Nanjing 211100, China

Corresponding author: Xianghui Han (han.xianghui@zte.com.cn)

ABSTRACT With new services emerging in fifth generation (5G)-advanced, the evolution in duplex modes plays an important role to meet more stringent requirements for both downlink (DL) and uplink (UL) transmissions. In this paper, sub-band full duplex (SBFD) at base station (BS) is studied as an attainable evolution of the traditional time division duplex (TDD). Both user equipment (UE) transparent SBFD and UE perceptive SBFD are proposed and studied to serve different types of UEs. To tackle the interference introduced by SBFD, a model including both BS self-interference and cross-link interference (CLI) is presented as a first step, and new interference management schemes are proposed. Three approaches to mitigate BS self-interference, namely the passive suppression, analog interference cancellation and digital interference cancellation are analyzed. A new framework for CLI management is illustrated along with enhancements for interference identification, spatial domain interference coordination and power domain adjustment. To validate the feasibility and performance of the proposed SBFD methods under indoor and dense urban scenarios, system-level simulations (SLSs) are carried out and a proof-of-concept (PoC) is developed for the purpose of obtaining experimental results.

INDEX TERMS 5G, full duplex, TDD, interference, prototype.

I. INTRODUCTION

The fifth generation (5G) networks are serving a growing number of end users and vertical industries, contributing to a smarter and more digitized society. In the previous releases, 5G standards mainly focus on services that require one particular requirement. For example, the enhanced mobile broadband (eMBB) services mainly require large bandwidths. On the other hand, system designs for the ultra reliable and low latency communication (URLLC) services focus on enhancements of low latency and high reliability [1], [2]. These services may coexist in many scenarios and require flexible scheduling by networks [3], [4]. The co-existence of different services with different needs requires advanced and flexible duplex methods.

Time division duplex (TDD) is specified as the duplex mode for 5G at operating bands higher than approximately 2 GHz [5]. TDD has the advantage of using one carrier with flexible uplink (UL) and downlink (DL) ratios to better meet asymmetric requirements for UL and DL. In addition, channel reciprocity can be used for channel state information (CSI) acquiring, so that the overhead associated with CSI reports can be significantly reduced especially when there is a large number of antennas [6]. However, the commercialized networks only support DL heavy TDD configuration, such as 4 DL slots and 1 UL slot for every TDD period, to support high throughput for DL. The limited allocation of time domain resources for UL results in reduced UL throughput and coverage as well as increased latency.

The associate editor coordinating the review of this manuscript and approving it for publication was Tiago Cruz.

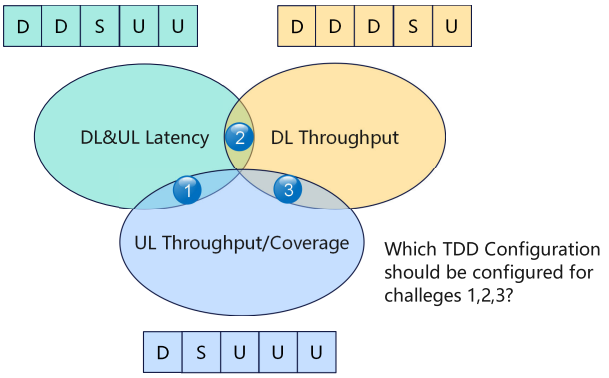

FIGURE 1. Challenges of conventional TDD operations.

In the first three releases of the third generation partnership project (3GPP) 5G new radio (NR) standards, many techniques have been exploited to enhance UL performance. For example, UL throughput can be improved by multiple-input multiple-output (MIMO) and carrier aggregation (CA). In Release 16 and 17, several solutions to reduce latency for URLLC services have been specified, such as mini-slot monitoring and scheduling. The Release 17 work item on coverage enhancement introduced some enhancements for UL channels including the physical uplink control channel (PUCCH), the physical uplink shared channel (PUSCH) and Message 3 (Msg3) [7]. It is also possible to adopt a dynamic resource allocation scheme for wireless networks providing different types of services [8]. However, as the diversity of 5G services continue to grow and evolve, higher and more comprehensive requirements for network performance are becoming a pressing matter. Three major challenges emerge with respect to how to satisfy more than one DL and UL requirements simultaneously has become the main challenges for the conventional TDD system [9]. As illustrated in Fig. 1, the first challenge is to ensure UL throughput and coverage and satisfy latency requirement for both DL and UL simultaneously. Machine vision, monitoring and sensing for safety use cases can be classified into this category. The second challenge is how to ensure DL throughput and satisfy latency requirement for both DL and UL simultaneously. Online gaming is one of the representative use cases for this challenge. The third challenge is ensuring DL throughput and UL throughput and coverage simultaneously, to support use cases such as extended reality (XR).

One effective approach to address above challenges is full duplex. By implementing full duplex at both the transmitter and receiver, DL and UL signals can be transmitted and received on overlapping time and frequency resources, which can double the spectral efficiency theoretically. In [10], the authors propose an in-band full duplex communication scheme to potentially double the spectral efficiency. The paper addresses the architectural considerations for real-time processing of wideband signals in full-duplex systems. It develops a least mean squares (LMS) based adaptive filter with an architecture integrated with subbanding and parallelization that processes data at 2 Gbps in real-time operating in 1 GHz of instantaneous bandwidth. However, the architecture might be cost-prohibitive for commercial wide-area deployment. In [11], the authors present a comprehensive list of the potential full duplex techniques and highlight their advantages and disadvantages. The survey focuses on self-interference techniques to address a range of critical issues related to the implementation, performance enhancement and optimization of full duplex systems. In [12], the authors propose an alternative sub-band approach for wideband self-interference cancellation in full-duplex transceiver. In the proposed approach, the emulated transmit signal and the desired signals at the receiver are divided into a number of sub-bands and the self-interference cancellation is performed at each of these sub-bands. In both [11] and [12], the proposed methods to mitigate self-interference are under in-band operation scenarios where transmissions and receptions are in fully overlapping resources in the frequency domain. In [13] and [14], the authors present the evaluation scenarios, use cases and simulation assumptions for sub-band non-overlapping full duplex in 5G-advanced. Interference modeling is also discussed while it does not provide the detailed analysis on how to mitigate the self-interference and CLI. In [15], the authors propose different frameworks of sub-band full duplex including sub-band based SBFD, bandwidth part (BWP) based SBFD and half duplex CA based SBFD CA, which all targets for the specification impacts in 3GPP.

There are some other literature addressing the high self-interference and cross-link interference (CLI) caused by in-band full duplex [16], [17], [18], [19], [20]. However, these techniques for in-band full duplex are too complicated to be widely implemented in real network deployment, and they can only be applicable for updated new user equipments (UEs). An alternative which can be implemented by the industry is non-overlapping sub-band full duplex (SBFD), which is proposed in 5G-advanced at base station (BS) side [21]. By using SBFD, an UL sub-band can be introduced within DL slots of a TDD period. In this way, UL reception and DL transmission can be performed simultaneously for a BS within a band across different sub-bands. Consequently, the BS can provide different UEs with different TDD configurations in different sub-bands to satisfy different requirements. For instance, UL heavy TDD configuration can be allocated to UEs requiring large UL coverage or high UL throughput, while DL heavy TDD configuration can be allocated to UEs to ensure high DL throughput. In [22], some general BS-to-BS CLI handling methods are presented. However, these methods are very high-level without any details and the focused scenario are dynamic TDD configurations instead of sub-band full duplex scenario. In [23], the authors propose some power domain enhancements for BS-to-BS CLI handling. The proposed methods are straightforward to simply increase the UE power or reduce BS power to mitigate the BS-to-BS CLI.

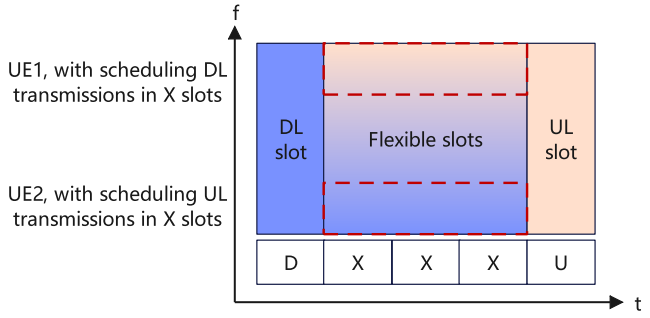

FIGURE 2. Example of UE transparent SBFD operation.

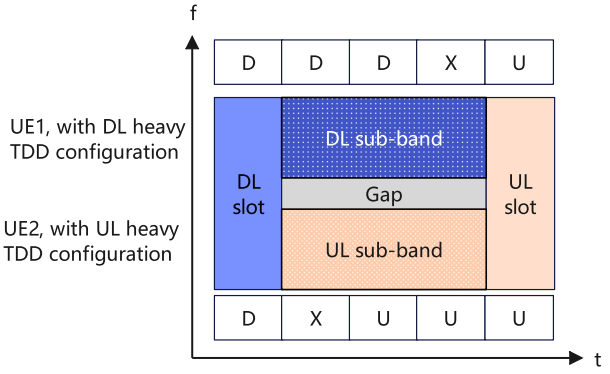

FIGURE 3. Example of UE perceptive SBFD operation.

Despite the advantages of SBFD, there are currently no detailed designs on how to support SBFD and how to handle the interference. This paper intends to fill in this gap. In this paper, both UE transparent SBFD and perceptive SBFD are proposed as the alternative solutions to serve different types of UEs. The model on interference is also provided, including both BS self-interference and CLI for different deployment scenarios, with new interference management schemes proposed accordingly. The performance of the proposed SBFD methods are evaluated by SLSs and tests on PoCs.

The rest of the paper is organized as follows. Section II introduces the system model including the SBFD mode and interference model. In Section III, Schemes for interference management for both self-interference and CLI are presented. Section IV provides the evaluation results based on both SLSs and PoCs. Finally, Section V concludes this paper.

II. SYSTEM MODEL

A. SBFD MODEL

1) UE TRANSPARENT SBFD OPERATION

Current conventional UE is able to support UL transmission or DL reception based on dynamic UL/DL scheduling in the flexible slots/symbols. With this, a UE transparent SBFD operation is proposed by configuring a set of flexible slots for the TDD configuration. This could allow conventional UEs to enjoy the enhanced performance without any update.

In Fig. 2, an example is shown with TDD UL/DL configuration of {DXXXU}, where 'D', 'X', 'U' is DL, flexible and UL slot respectively. For UE1 requiring high DL throughput, DL transmission can be scheduled in the flexible slots. For UE2 in cell edge or requiring high UL throughput, UL transmission can be scheduled instead. In these flexible slots, BS needs to support full duplex by maintaining both DL transmission and UL reception simultaneously, while UE1 and UE2 are still in half duplex mode with legacy TDD operation. Such kind of scheduling would cause self-interference and CLI, which are discussed in the subsequent sections.

2) UE PERCEPTIVE SBFD OPERATION

Another alternative SBFD operation is to let BS configure specific sub-band information to UEs. The main advantage is to allow more aligned sub-band configuration among BSs which could reduce the CLI.

An example is shown Fig. 3, where one DL sub-band, one frequency gap, one UL sub-band are configured in the three middle slots of one TDD configuration period. The gap is used to reduce the self-interference from DL sub-band to UL sub-band. TDD configuration 'DDDXU' can be assigned to accommodate high DL throughput for UE1. For UE2 in cell edge or requiring high UL throughput, 'DXUUU' can be assigned instead. Similarly, BS needs to support full duplex by maintaining both DL transmission and UL reception simultaneously. UE1 and UE2 are still in half duplex mode with legacy TDD operation, while should be able to interpret the sub-band information.

B. INTERFERENCE MODEL

The SBFD operations at the BS will introduce new types of interference which need to be defined. Three types of new interference are specified below respectively.

- BS inter-sub-band self-interference: UL reception of a BS in one sub-band is interfered by DL transmission of the BS in another sub-band during a same time interval.
- Inter-BS inter-sub-band interference: UL reception of a BS in one sub-band is interfered by DL transmission of another BS in another sub-band during a same time interval.
- Inter-BS intra-sub-band interference: UL reception of a BS in one sub-band is interfered by DL transmission of another BS in a same sub-band during a same time interval.

Note that the inter-UE interference is typically smaller than inter-BS interference due to the lower transmission power of UEs. In this section, we focus on the aforementioned three types of interference at BS side only, under two specific deployment scenarios as follows.

1) SAME RESOURCE CONFIGURATION SHARING AMONG ADJACENT BSs

As an example shown in Fig. 4, assuming the UL and DL resources of adjacent BSs are aligned with each other by sharing a same frame structure configuration and full duplex scheduling/configuration. Considering the performance of

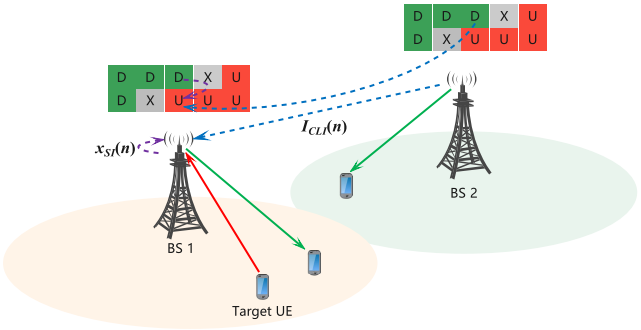

FIGURE 4. Inter-sub-band co-channel CLI.

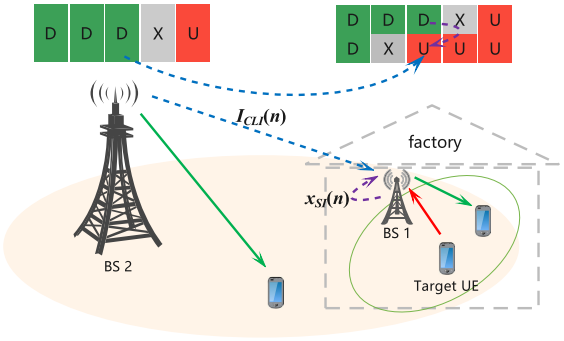

FIGURE 5. Intra-sub-band co-channel CLI.

UL reception in the UL sub-band by BS from target UE, the new interference type caused by the introduction of SBFD comes from inter-sub-band. More specifically, the inter-sub-band interference includes two parts: (1) BS1 self-interference (shown in purple dotted line) and (2) inter-BS inter-sub-band interference from aggressor BS2 (shown in blue dotted line). As the two BSs operating at the same frequency band, the inter-BS inter-sub-band interference is co-channel interference.

Let $x_{g1}(n)$ be the baseband signal transmiting at time sample n. The non-linear power amplifier (PA) output signal $x_{PA,g1}(n)$ can be expressed using a proper non-linear models. For simple PA models, one can use the Rapp model, Saleh model and the Ghorbani model [24], [25], [26]. Combinations of pure polynomial models and filter models are also often referred to as fairly simple models, of which the Hammerstein model is one representative [27]. A more rigorous and comprehensive model is the Volterra series expansion model which can model all weak non-linearity with fading memory [28]. A subset of the Volterra series is the memory polynomial model [29], [30] with polynomial representations in several delay levels. The generalized memory polynomial (GMP) model is easily implemented by modeling the PA with realistic parameters. Here, a modified GMP model is used and the PA output signal $x_{PA,g1}(n)$ can be expressed as

$$\begin{aligned} &x_{PA,g1}(n) \\ &= \sum_{k\in K_a}\sum_{l\in L_a} a_{kl}x_{g1}(n-l)\left|x_{g1}(n-l)\right|^{2k} \\ &\quad + \sum_{k\in K_b}\sum_{l\in L_b}\sum_{m\in M} b_{klm}x_{g1}(n-l)\left|x_{g1}(n-m)\right|^{2k}, \end{aligned} \quad (1)$$

where $x_{g1}(n)$ represents the complex baseband equivalent input of the model. The first term represents the double sum of so called diagonal terms where the input signal at time shift l. $x_{g1}(n-l)$ is multiplied by different orders of the time aligned input signal envelope $\left|x_{g1}(n-l)\right|^{2k}$, $k \in K_a$. The triple sum represents cross terms, i.e. the input signal at each time shifts is multiplied by different orders of the input signal envelope at different time shifts. The GMP is linear in the coefficients, a_{kl} and b_{klm}, which caters for robust estimation based on input and output signal waveforms of the PAs to be characterized.

The BS inter-sub-band self-interference $x_{SI}(n)$ at the receiver (Rx) chain can be given as

$$x_{SI}(n) = h_{cop}(n) \otimes x_{PA,g1}(n), \quad (2)$$

where $h_{cop}(n)$ is the coupling response from transmitter (Tx) chain to Rx chain at time sample n.

The inter-BS inter-sub-band CLI from BS2 to BS1 can be expressed as

$$I_{CLI}(n) = h_{cli} \otimes x_{PA,g2}(n), \quad (3)$$

where $x_{PA,g2}(n)$ is the transmit signal after PA from BS2 and $h_{cli}(n)$ is the impulse response of the channel between BS1 and BS2.

Then, the received signal $y(n)$ at BS1 can be expressed as

$$y(n) = h_x(n) \otimes x(n) + x_{SI}(n) + I_{CLI}(n) + z(n), \quad (4)$$

where $x(n)$ is the desired transmit signal by the target UE and $h_x(n)$ is the impulse response of the channel between BS1 and the target UE. $z(n)$ is the additive Gaussian random noise.

In Section III, interference management is discussed to cancel or reduce the self-interference $x_{SI}(n)$ and CLI $I_{CLI}(n)$.

2) DIFFERENT RESOURCE CONFIGURATIONS FOR ADJACENT BSs

Another typical deployment is showed in Fig. 5, a macro BS with DL-dominant TDD configuration (e.g., DDDXU) is deployed outside a factory, which is covered by an indoor small cell with UL-dominant SBFD configuration, i.e., UL sub-band are configured during three middle slots.

Compared to the interference scenario shown in Fig. 4, the main difference of interference model of the co-existence scenario shown in Fig. 5 is $I_{CLI}(n)$, for which it is intra-sub-band co-channel interference when BS2 operating at the same band with BS1 or inter-band adjacent channel interference when BS2 operating at a different band.

III. INTERFERENCE MANAGEMENT FOR SBFD

A. SELF-INTERFERENCE MANAGEMENT

As described in Section II-B, self-interference is one of the main interferences in SBFD system. To enjoy the performance gain of SBFD, it is crucial to mitigate the impact

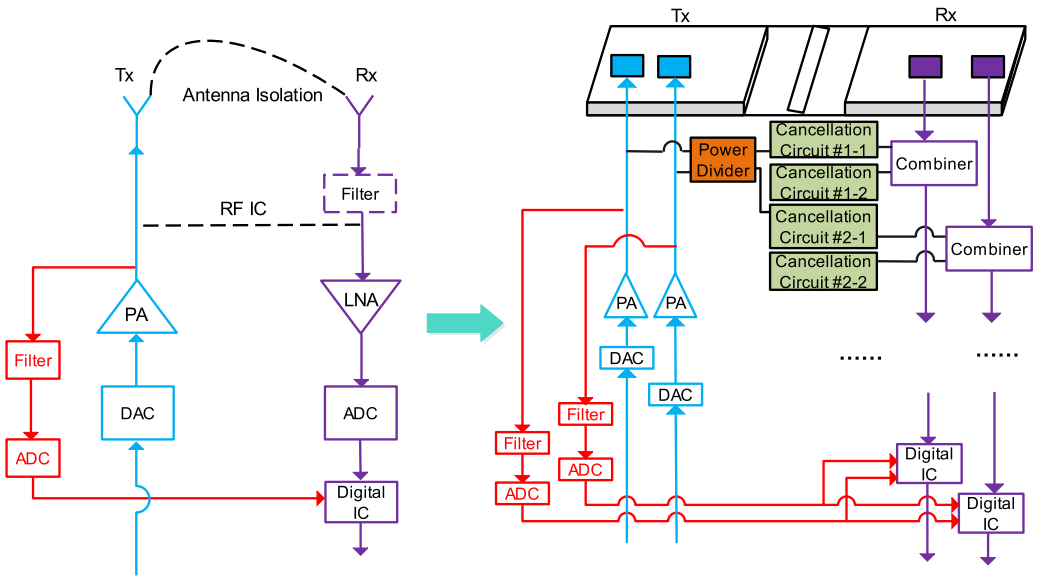

FIGURE 6. Schemes for self-interference cancellation.

of self-interference. Overall, techniques to mitigate the self-interference can be divided into three categories, namely, passive suppression, analog interference cancellation (IC) and digital IC.

1) PASSIVE SUPPRESSION

Passive suppression mainly includes antenna isolation and beam forming. In the conventional TDD system, Tx antennas and Rx antennas of the base station are in the same panel. Typically, Tx and Rx share the same antennas in order to achieve the channel reciprocity at the base station side. However, if base station uses the same antenna for Tx and Rx or if the Tx antennas and Rx antennas are close to each other (e.g., in the same panel), it will cause serve self-interference. Thus, to mitigate the self-interference, the Tx antennas and Rx antennas can be arranged in different panels to achieve the antenna isolation [17], [31]. The achievable antenna isolation highly depends on the distance between Tx and Rx antennas, i.e., the greater distance, the higher antenna isolation. However, greater distance may have negative impact on the cost and form factor of Active Antenna Unit (AAU). Typically, the antenna isolation is around 45 dB between Tx and Rx antennas at the base station side [17], [32]. To further increase the antenna isolation between Tx and Rx antennas, one or multiple walls can be deployed in between of the Tx antennas and Rx antennas. With walls in between, the antenna isolation can be increased to around 55 dB. As depicted in Fig. 6, the Tx antennas and Rx antennas are in two separate panels with a wall in between.

Beam forming is introduced in the Multiple Input Multiple Output (MIMO) system to make the signal transmitted in a narrow direction. With beam forming, base station adjusts the Tx beam and Rx beam to mitigate the self-interference.

2) ANALOG CANCELLATION

Analog cancellation mainly contains radio frequency (RF) interference cancellation and analog filter. RF interference cancellation mitigates the self-interference via RF cancellation circuits. The RF cancellation circuits transfer the transmission signal to the receiver and allow the receiver to eliminate the interference signal (i.e., the leakage from the transmission signal). Since the transmission signal over each Tx antenna needs to be transferred to each Rx antenna, the cost and complexity of RF cancellation circuits increases a lot in case of large number of antennas. Assuming the number of Tx antennas and Rx antennas are M and N, respective, $M \cdot N$ RF cancellation circuits are required. Thus, the target use case for RF interference cancellation is base stations with smaller number of Tx and Rx antennas, e.g., Pico cells.

In SBFD system, sub-band analog filter provides further isolation between the transmitter and receiver. According to research [33], analog filter can provide around 30 dB isolation between the transmitter and receiver. Compared with RF cancellation circuits, the complexity of analog filter is reduced since the number of filters is equal to the number of Rx antennas. Assuming the number of Tx antennas and Rx antennas are M and N, respective, only N sub-band analog filters are required. In SBFD system, the bandwidth of analog filter is not able to be changed flexibly. This will further reduce the configuration flexibility of SBFD. In addition, the sub-band analog filter also cause insertion loss in the RF chain. The UL performance may be reduced due to this insertion loss.

3) DIGITAL CANCELLATION

Digital cancellation refers to methods to mitigate the self-interference in digital domain. In order to counteract the PA non-linearities, digital pre-distortion (DPD) is widely

applied in commercial transmitters. Another approach is to implement digital cancellation after the baseband signal is possessed through the digital to analog converter (DAC) and PA as shown in Fig. 6, where the leakage signal from the transmission side is transformed to digital signal via the analog to digital converter (ADC) and transferred to the receiver to perform digital interference cancellation. Since the leakage signal going into the receiver has been experienced the channel between the transmitter and receiver, reference signal may be needed for the receiver to estimate the channel between the transmitter and receiver. In addition, the non-linearity of the sub-band filter and low-noise amplifier (LNA) at receiver also impacts the performance of digital interference cancellation.

B. CLI MANAGEMENT

To reduce the impact of CLI, an enhanced framework for CLI management among with several techniques to identify and mitigate the CLI is presented in this subsection.

1) FRAMEWORK

As depicted in Fig. 7, an enhanced framework is proposed for CLI management between victim BS and aggressor BS. The interaction procedures for the proposed framework are summarized below.

- Step 0: The victim identifies inter-BS interference basing on measurement of transmission from the aggressor.
- Step 1: The victim indicates information identified from Step 0, e.g., cell/beam information with high interference strength, via either reference signal (RS)-1 or backhaul.
- Step 2: The victim starts to monitor RS-2 from the aggressor once it transmits the interference indication in Step 1, though the aggressor may not start to transmit RS-2 yet.
- Step 3: The aggressor performs interference mitigation solutions based on the indication from victim in Step 1.
- Step 4: The aggressor transmits RS-2, which is used to assist the victim to decide whether/which solution can mitigate the inter-BS interference effectively. For example, RS-2 are transmitted on a group of resources with different powers or different beams, which corresponds to different interference mitigation solutions.
- Step 5: The victim determines which interference mitigation solution can mitigate the interference effectively through RS-2 measurement and transmit interference mitigation indication to the aggressor.

2) INTERFERENCE IDENTIFICATION

The main purpose of interference identification is to determine the high-interference BS (aggressor) as well as the high-interference beam. Further, the CSI for the interference channel can also be obtained through the estimation of measured RSs. Regarding the intra-sub-band co-channel interference, synchronization signal block (SSB) or CSI-RS can be used as measurement RS, and Reference Signal

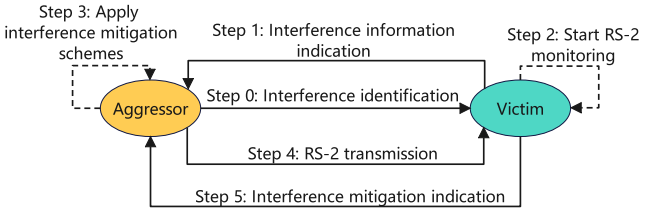

FIGURE 7. Framework for inter-BS CLI management.

Receiving Power (RSRP) measurement can be defined for the interference identification. While for inter-sub-band co-channel interference, the received signal strength indicator (RSSI) measurement on some specific resources can be defined to identify the interference power leaked from adjacent DL sub-band.

Accurate interference measurement is the prerequisite for interference management. When the victim performs the inter-BS CLI measurement, it cannot perform the DL transmission on the measurement resources to prevent the transmission from affecting its own measurement. In addition, it is also better for the victim not to perform the UL reception on the measurement resources for more accurate measurement. For UL transmission (e.g., PUSCH, Sounding RS, etc) at UE side, a rate matching mechanism can be introduced. That is, defining one or more time-frequency resource patterns, in which the resource is unavailable for the UL transmission. The time-frequency domain resource pattern can be indicated via time-frequency domain configuration of SSB, CSI-RS or resources for RSSI measurement. In addition, a frequency-domain guard band should also be considered to avoid the impact of adjacent-frequency interference on the measurement.

For RSRP measurement, timing alignment between the aggressor and the victim is a key aspect to take into account for obtaining an accurate time-domain resource for measuring and rate matching. As shown in Fig. 8, there are mainly two factors. One is the timing difference between the aggressor and the victim, which is marked as T1 in Fig. 8. Another factor is transmission time from the aggressor to the victim, which is mark as T2. An example for determination of the measurement resource and the rate matching resource is shown in Fig. 9. More specifically, both of T1 and T2 are taken into account for determining the time domain resource of the measurement and the rate matching. In addition, a larger bandwidth is configured for rate matching than that of measurement resources, and the frequency-domain guard band is reserved to reduce the impact of adjacent-frequency interference on the measurement.

3) SPATIAL DOMAIN INTERFERENCE COORDINATION

Spatial domain interference coordination is a promising mode for interference mitigation. The victim identifies the beam with high interference of the aggressor according to the measurement, and feeds back the beam information to the aggressor in the Step 1. For example, assuming the

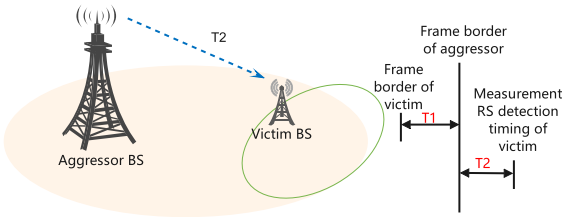

FIGURE 8. Timing alignment between the aggressor and the victim.

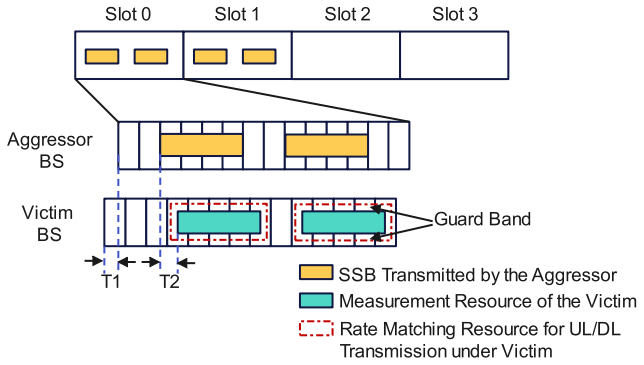

FIGURE 9. Determination of the measurement resource and the rate matching resource.

SSB is used as the measurement RS, and the predefined interference threshold is $I_{threshold}$. All the SSBs with SSB-RSRP higher than $I_{threshold}$ will be fed back. That is, the feedback information includes a group of SSB indexes and the SSB-RSRP value corresponding with each SSB index. After the aggressor receives the feedback information of the high interference beams, it will restrict the time-frequency domain resources for transmission using the high-interference beams. For example, DL transmission with high-interference beam cannot use the time-domain resources configured with UL sub-band. Alternatively, the victim can measure the interference channel and feed back the channel state information to the aggressor, the beamforming of the DL transmission from the aggressor can be adjusted by considering the channel state information of the interference channel.

4) POWER DOMAIN ADJUSTMENT FOR INTER-SUB-BAND INTERFERENCE SUPPRESSION

It is proposed to introduce a power adjustment factor to change UL transmission power so as to neutralize the impact from inter-sub-band interference.

As an example shown in Fig. 10, the inter-sub-band interference can be described by a piece-wise linear function. For example, the interference value at a target point (e.g., A_0) can be determined according to the interference value at a reference point (e.g., the spectrum edge of DL sub-band, i.e., A_1 to A_2) and frequency offset between the target point and the reference point.

Take the inter-sub-band interference caused by low-frequency DL sub-band to UL sub-band for example.

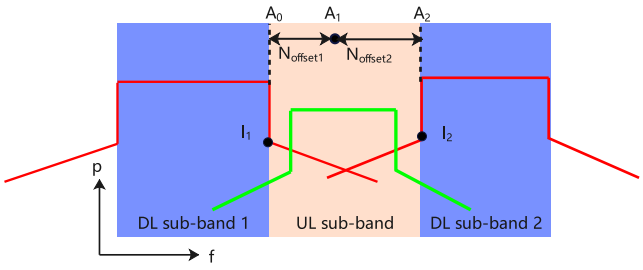

FIGURE 10. Inter-sub-band interference.

TABLE 1. Example of relationship between I_{total} and O.

I_{total} (dBm)	O (dB)
$0 \le I_{total} < I_{threshold1}$	2
$I_{threshold1} \le I_{total} < I_{threshold2}$	4
$I_{threshold2} \le I_{total}$	6

Suppose the interference quantity leaked from low-frequency DL sub-band at the reference point A_1 is I_1 dBm. The interference quantity is decreased by k_1 dB per frequency unit. Then, the interference quantity at the target frequency point A_0, which is, $N_{offset1}$ frequency units away from the reference point, is: $I_{low} = I_1 - k_1 N_{offset1}$.

Similarly, the interference caused by the high-frequency DL sub-band to the UL sub-band: $I_{high} = I_2 - k_2 N_{offset2}$, where I_2 is the interference leaked by the high-frequency DL sub-band at the reference point A_2, $N_{offset2}$ is the number of frequency unis between the target frequency point A_0 and the reference point A_2, and k_2 is the dB quantity of interference amount decreased per frequency unit.

Then, at the target frequency point A_0, the total quantity of inter-sub-band interference from both sides is: $I_{total} = I_{low} + I_{high}$. And the relationship between power adjustment factor (O) and total quantity of inter-sub-band interference I_{total} can be defined as an example shown in Table 1. Based on the value range of I_{total}, a UE can get the corresponding O. For calculation of I_{total}, BS needs to indicate the following parameters for the UE: I_1, k_1, I_2 and k_2.

For I_{total} calculation, a reference physical resource block (PRB) within the UL transmission can be selected as the target frequency point, e.g., the central PRB of the UL transmission.

5) POWER DOMAIN ADJUSTMENT FOR INTRA-SUB-BAND INTERFERENCE SUPPRESSION

For intra-sub-band interference causing by transmission from aggressors in the overlapping sub-band, the interference levels on different resources sets may be different. One way to accommodate this is to make each set of resources mapped with a dedicated power control parameter set. The power control parameters set could contain either open-loop power control parameter, e.g., $P0$, *alpha*, or closed-loop power control parameter, e.g., transmission power control (TPC) table.

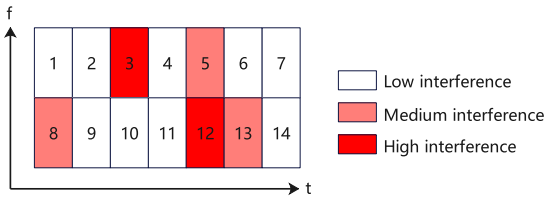

FIGURE 11. Different interference levels on different resource sets.

TABLE 2. Example of relationship between resource sets and open-loop power control parameters sets.

Resource Set	Open-loop power control parameters set
The first resource set	$\{P0, alpha\}\#1$
The second resource set	$\{P0, alpha\}\#2$
The third resource set	$\{P0, alpha\}\#3$

As an example shown in Fig. 11 and Table 2, the relationship between resource sets and open-loop power control parameter sets is defined. In this example, there are $N = 3$ open-loop power control parameter sets are defined, i.e., $\{P0, alpha\}\#1$, $\{P0, alpha\}\#2$ and $\{P0, alpha\}\#3$, which are associated with three sets of resource (i.e., the first resource set with low interference, the second resource set with medium interference and the third resource set with high interference, respectively.

Based on the actual scheduling resources of a UE, it uses a corresponding open-loop power control parameters sets for determination of UL transmission power.

IV. EVALUATION AND NUMERICAL RESULTS

A. SYSTEM LEVEL SIMULATIONS

In this subsection, SLSs for SBFD operation are conducted in both indoor hotspot and dense urban scenarios. In Fig. 12, the flowchart of SLS for the proposed SBFD operation with simultaneously generating DL and UL traffic in the system is presented. In this paper, we focus on inter-BS interference so that the interference modeling is added in the module of 'Uplink Measurement and Interference Modelling' to evaluate the interference impact on UL reception at victim BS. The proposed methods for CLI interference management, they can be implemented at the aggressor BS to adjust the DL transmission or victim BS to adjust the scheduling of UL transmission.

In the evaluation, separate antenna panels are used for DL transmission and UL reception in slots with SBFD operation. For legacy TDD, static TDD UL/DL configuration with {DDDXU} is used, and the 'X' slot consists of 12 DL symbols, 2 gap symbols and 2 UL symbols. For SBFD operation, TDD UL/DL configuration with {XXXXU} is applied. In the time domain, UL sub-band spans all the symbols in a 'X' slot. In the frequency domain of the 'X' slot, the frequency band is divided into 104 PRBs for DL at one edge of the band, 53 PRBs for UL sub-band in the band center, and 104 PRBs for DL at another edge of the band, with 6 PRBs for gap between DL and UL. Other SLS assumptions are given in Table 3.

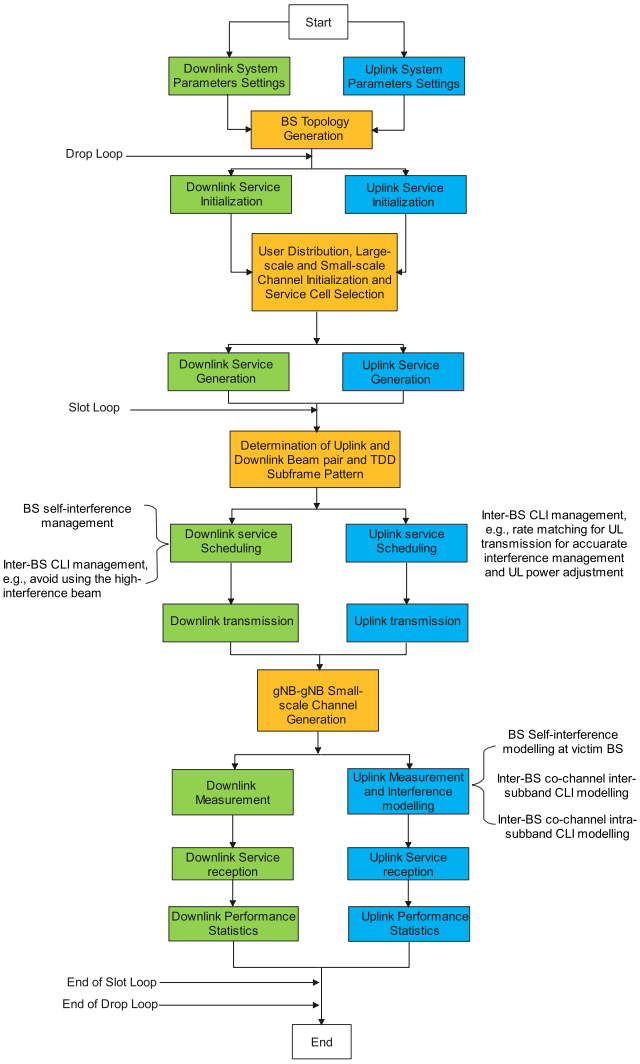

FIGURE 12. Flowchart of SLS for the proposed SBFD operation.

The DL and UL throughput performances as well as latency distributions for indoor hotspot scenarios are shown from Fig. 13 to Fig. 16 under different settings of DL/UL arrival rate λ_d/λ_u for traffic model. By enabling SBFD operation, we observe that the UL performance in terms of mean user perceived throughput (UPT) increases about 164% and 255% for $\lambda_d/\lambda_u = 10/1.25$ and 2.5/1.25 respectively. On the other hand, the mean DL UPT degrades about 24.7% and 39.6% for $\lambda_d/\lambda_u = 10/1.25$ and 2.5/1.25 respectively. In addition, the UL latency for SBFD is reduced significantly while the DL latency degradation can be acceptable.

Based on the simulation results, a lower BS self-interference and inter-BS interference can be expected for the low DL resource utilization (RU) case, in which the UL performance gains for SBFD are more obvious. Therefore, from the perspective of maximizing UL performance, configuring SBFD under the low DL RU case is a better choice. On the

TABLE 3. SLS assumptions for SBFD evaluation.

Parameter	Indoor hotspot	Dense urban
Layout	Factory hall size: 120x50 m	Macro layer: Hex. Grid Micro layer: - Number of micro BSs per macro cell: 3 - All micro BSs are outdoor. As a layout of macro cell, 7 macro cites, 3 sectors per site model with wrap around
Carrier frequency	4 GHz	
System bandwidth	100 MHz	
Subcarrier spacing	30 KHz	
Inter site distance	20 m	200 m
Minimum BS-UE (2D) distance	0 m	Macro-to-UE: 35 m Micro-to-UE: 10 m
Minimum UE-UE (2D) distance	1 m (TR38.828)	3 m (TR36.843)
BS antenna height	3 m	Macro cells: 25 m; Micro cells: 10 m;
TxRU mapping	Per panel, reuse models in TR36.897. A single TxRU is mapped per panel per polarization.	
BS antenna configuration	2 Tx/2 Rx antenna ports. (M, N, P, Mg, Ng; Mp, Np) = (4, 4, 2, 1, 1; 1, 1) for legacy TDD; (M, N, P, Mg, Ng; Mp, Np) = (4, 4, 2, 1, 2; 1, 1) for SBFD; (dH,dV)=(0.5,0.8)λ	
UE antenna configuration	2 Tx/2 Rx antenna ports. Mg = 1, Ng = 1, P = 2, d_H = 5 (M, N, P, Mg, Ng; Mp, Np) = (1, 1, 2, 1, 1; 1, 2);	
BS TX power	24 dBm per 20 MHz	33 dBm per 20 MHz based on TR38.802
UE Tx power	23 dBm	
UE power control	P0 = -60 dBm alpha = 0.6	P0 = -80 dBm alpha = 0.8
Noise	BS: 5 dB, UE: 9 dB	
UE density	10 UEs per transmission and reception point (TRxP)	
Self-interference suppression	130 dB	
CLI	Adjacent channel interference power ratio ACIR BS-BS: 45 dB. ACIR BS-UE: 33 dB. ACIR UE-BS: 30 dB. ACIR UE-UE: 28 dB.	

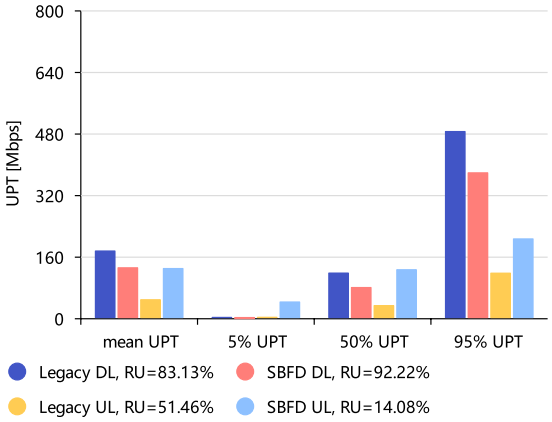

FIGURE 13. Throughput performance for indoor hotspot scenarios with λ_d/λ_u = 10/1.25.

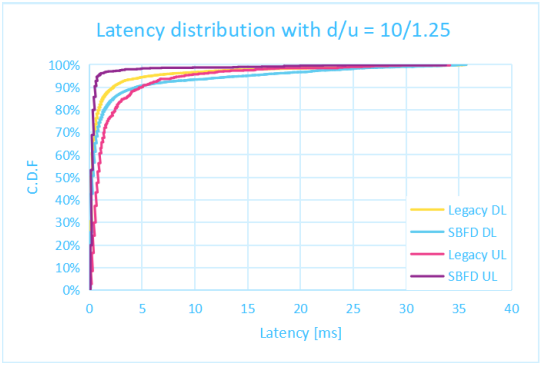

FIGURE 14. Latency distributions for indoor hotspot scenarios with λ_d/λ_u = 10/1.25.

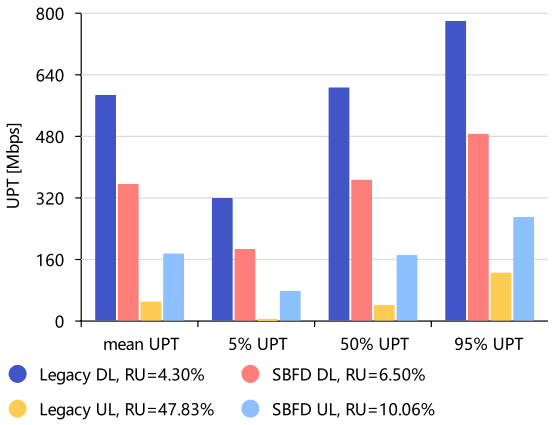

FIGURE 15. Throughput performance for indoor hotspot scenarios with λ_d/λ_u = 2.5/1.25.

other hand, from the perspective of minimizing the impact on DL performance, it is better to configure SBFD in the high DL RU case. For SBFD operation, some scheduling optimization can also be considered, e.g., X slot only schedules UEs at the center of the cell so as to avoid UL service congestion and reduce UL RU significantly.

The DL and UL throughput performances as well as latency distributions for dense urban scenarios are shown from Fig. 17 to Fig. 20 under different settings of λ_d/λ_u. Similarly, as can be seen from the simulation results, although the performance degradation for DL throughput is observed, the performance improvements for UL are significant in terms of both throughput and latency, especially for micro UEs. More specifically, for UEs in the macro layer, the mean UL UPT performance gain for SBFD is about 57.7% and 24.2% for λ_d/λ_u = 5/2.5 and 2.5/1.25 respectively, while the mean DL UPT degradation for SBFD is about 38.6%

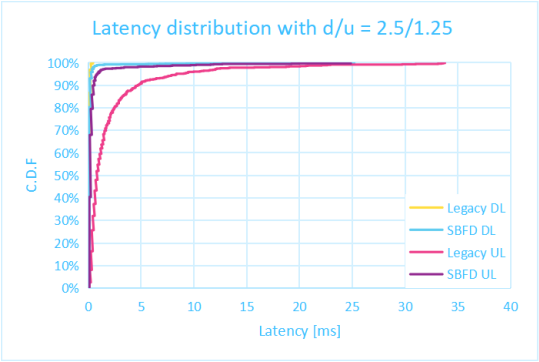

FIGURE 16. Latency distribution for indoor hotspot scenarios with $\lambda_d/\lambda_u = 2.5/1.25$.

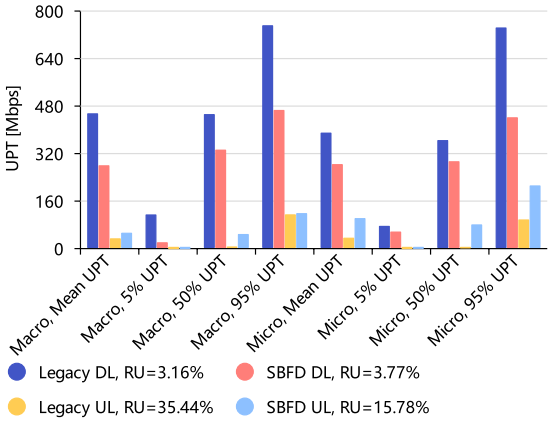

FIGURE 17. Throughput performance for dense urban scenarios with $\lambda d/\lambda u = 5/2.5$.

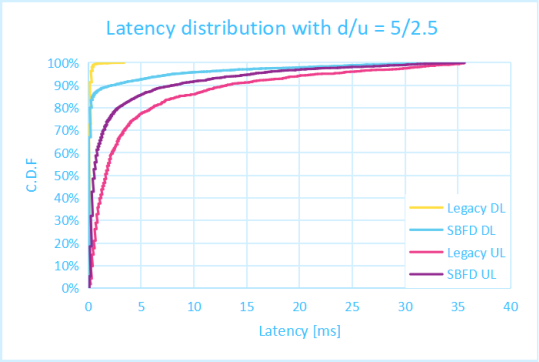

FIGURE 18. Latency distribution for dense urban scenarios with $\lambda_d/\lambda_u = 5/2.5$.

and 36.4% for $\lambda_d/\lambda_u = 5/2.5$ and 2.5/1.25 respectively. For UEs in the micro layer, the mean UL UPT performance gain for SBFD is about 188% and 128% for $\lambda_d/\lambda_u = 5/2.5$ and 2.5/1.25 respectively, while mean DL UPT is only degraded about 27.3% and 26.1% for $\lambda_d/\lambda_u = 5/2.5$ and 2.5/1.25 respectively. Regarding the latency performance, the UL latency is reduced significantly while the DL latency degradation can be acceptable.

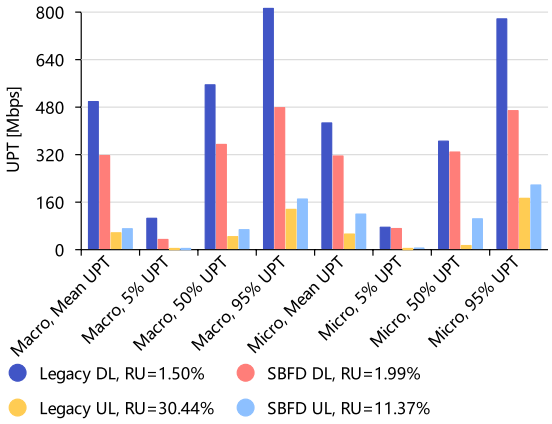

FIGURE 19. Throughput performance for dense urban scenarios with $\lambda d/\lambda u = 2.5/1.25$.

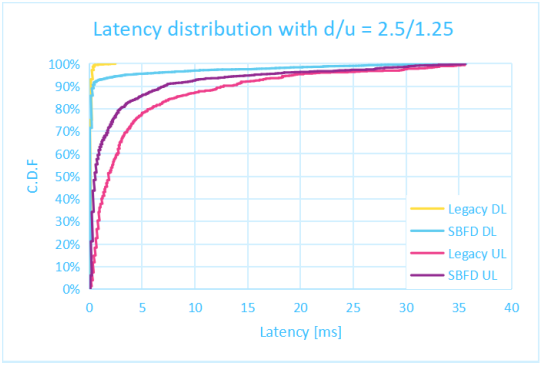

FIGURE 20. Latency distribution for dense urban scenarios with $\lambda_d/\lambda_u = 2.5/1.25$.

B. PoC EVALUATION

In this paper, a PoC is implemented to evaluate the actual performance of the proposed SBFD operation. The PoC comprises of two main parts, the remote radio unit (RRU) of the BS as shown in Fig. 21(a) and the legacy baseband unit (BBU) with software upgrades only as shown in Fig. 21(b). The test UE (TUE) used for PoC evaluation is also shown in Fig. 21(b).

The basic parameters about the prototype are provided in Table 4, wherein the 130 dB self-interference capability includes 55 dB antenna isolation, 45 dB Adjacent Channel Leakage Ratio (ACLR) and 30 dB sub-band filtering and digital cancellation.

The real-time end-to-end (E2E) round trip latency and the peak data rate obtained from the tests using the developed PoC are illustrated in Fig. 22 and Fig. 23 respectively. Fig. 22 shows that the E2E latency is always below 4 ms, with an average value of 3.9 ms. This shows that the E2E latency is quite stable and can be contained within a small range. This is mainly achieved by changing the frame structure dynamically for SBFD slots to accommodate the variation of arrival time for each packet. The UL data rate, as reflected by Fig. 23, is always higher than 1.4 Gbps. This is not only due to

(a)

(b)

FIGURE 21. The PoC developed in this paper comprises of (a) the RRU, and (b) the BBU and 5G TUE.

TABLE 4. Basic parameters of the prototype.

Item	Setting
RRU frequency band	4.9 GHz
BS antenna configuration	4T4R
UE antenna configuration	4T4R
Packeg Size	360(H)*441(W)*70(D)
Power	4*250 mV
SBFD configuration	DXXXU
BBU system bandwidth	Non-SBFD slot: 100 MHz SBFD slot: 10 MHz for DL and 90 MHz for UL
Antenna isolation	21.5 cm
Self-Interference capability	130 dB

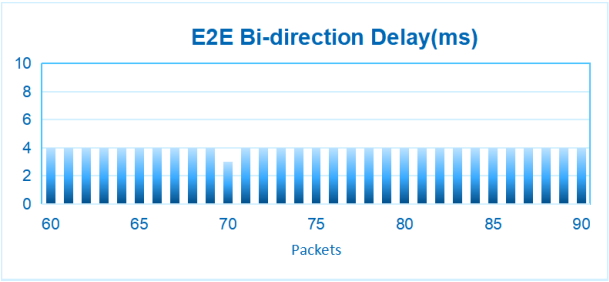

FIGURE 22. Test results obtained by the PoC for E2E latency.

more UL resources allocated and the advanced interference management proposed in this paper, but also some scheduling enhancement by implementation. For instance, the DL sub-band in a SBFD slot can across schedule an UL transmission in an UL sub-band in another SBFD slot. Overall, the test

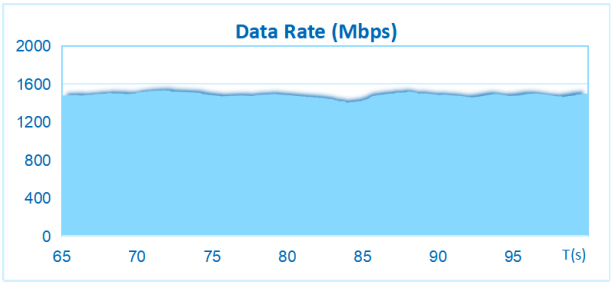

FIGURE 23. Test results obtained by the PoC for UL data rates.

results of the implemented PoC not only prove the feasibility of the SBFD for BS but also outline the reliable performance it can offer.

V. CONCLUSION

To better support service transmission with multi-dimensional requirements, a SBFD network with efficient interference management schemes is proposed. Specifically, interference model of the new interference type under SBFD is presented for different deployment scenarios, and new interference management schemes are further proposed for addressing these interference. For BS self-interference, passive suppression, analog interference cancellation and digital interference cancellation are analyzed. A new framework for CLI management through spatial domain and power domain is illustrated. Evaluations based on both a PoC and SLSs are conducted, both showing significant performance gains in different scenarios. As a next-step work plan, the SBFD network with proposed CLI management mechanisms will be further validated under more scenarios and configuration, such as, urban macro scenario, dense urban with different resource configurations for adjacent BSs, etc.

REFERENCES

[1] *IMT Vision: Framework and Overall Objectives of the Future Development of IMT for 2020 and Beyond*, Int. Telecommun. Union-Radio Commun. Sector (ITU-R), Geneva, Switzerland, 2015.

[2] R. Qi, X. Chi, L. Zhao, and W. Yang, "Martingales-based ALOHA-type grant-free access algorithms for multi-channel networks with mMTC/URLLC terminals co-existence," *IEEE Access*, vol. 8, pp. 37608–37620, 2020.

[3] M. Alsenwi, N. H. Tran, M. Bennis, A. K. Bairagi, and C. S. Hong, "EMBB-URLLC resource slicing: A risk-sensitive approach," *IEEE Commun. Lett.*, vol. 23, no. 4, pp. 740–743, Apr. 2019.

[4] A. Anand, G. De Veciana, and S. Shakkottai, "Joint scheduling of URLLC and eMBB traffic in 5G wireless networks," in *Proc. IEEE Conf. Comput. Commun. (INFOCOM)*, Apr. 2018, pp. 1970–1978.

[5] *Study on Channel Model for Frequencies From 0.5 to 100 GHz*, document TR38.901, 2022. [Online]. Available: https://portal.3gpp.org/desktopmodules/Specifications/SpecificationDetails.aspx?specificationId=3173

[6] J. Jose, A. Ashikhmin, T. L. Marzetta, and S. Vishwanath, "Pilot contamination and precoding in multi-cell TDD systems," *IEEE Trans. Wireless Commun.*, vol. 10, no. 8, pp. 2640–2651, Aug. 2011.

[7] *Study on nr coverage enhancements*, document TR 38.830, 2020. [Online]. Available: https://www.3gpp.org/DynaReport/38830.htm

[8] X. Han, K. Xiao, R. Liu, X. Liu, G. C. Alexandropoulos, and S. Jin, "Dynamic resource allocation schemes for eMBB and URLLC services in 5G wireless networks," *Intell. Converged Netw.*, vol. 3, no. 2, pp. 145–160, Jun. 2022.

[9] N. Khiadani, "Vision, requirements and challenges of sixth generation (6G) networks," in *Proc. 6th Iranian Conf. Signal Process. Intell. Syst. (ICSPIS)*, Dec. 2020, pp. 1–4.
[10] K. S. Lorenz, J. Goodman, M. Mcbeth, M. B. Mckeon, and D. J. Parrett, "A real-time wideband subband LMS algorithm for full-duplex communications," *IEEE Access*, vol. 10, pp. 32566–32573, 2022.
[11] Z. Zhang, K. Long, A. V. Vasilakos, and L. Hanzo, "Full-duplex wireless communications: Challenges, solutions, and future research directions," *Proc. IEEE*, vol. 104, no. 7, pp. 1369–1409, Jul. 2016.
[12] M. Ghoraishi, W. Jiang, P. Xiao, and R. Tafazolli, "Subband approach for wideband self-interference cancellation in full-duplex transceiver," in *Proc. Int. Wireless Commun. Mobile Comput. Conf. (IWCMC)*, Aug. 2015, pp. 1139–1143.
[13] *Discussion on Evaluation on NR Duplex Evolution*, document R1-2204303, 2022. [Online]. Available: https://portal.3gpp.org/ngppapp/CreateTdoc.aspx?mode=view&contributionId=1323065
[14] *Deployment Scenario and Evaluation Methodology for Duplex Evolution*, document R1-2203903, 2022. [Online]. Available: https://portal.3gpp.org/ngppapp/CreateTdoc.aspx?mode=view&contributionId=1322298
[15] *Discussion of Subband Non-Overlapping Full Duplex*, document R1-2203204, 2022. [Online]. Available: https://portal.3gpp.org/ngppapp/CreateTdoc.aspx?mode=view&contributionId=1320052
[16] T. Riihonen, S. Werner, and R. Wichman, "Mitigation of loopback self-interference in full-duplex MIMO relays," *IEEE Trans. Signal Process.*, vol. 59, no. 12, pp. 5983–5993, Dec. 2011.
[17] E. Everett, A. Sahai, and A. Sabharwal, "Passive self-interference suppression for full-duplex infrastructure nodes," *IEEE Trans. Wireless Commun.*, vol. 13, no. 2, pp. 680–694, Jan. 2014.
[18] S. Hong, J. Brand, J. I. Choi, M. Jain, J. Mehlman, S. Katti, and P. Levis, "Applications of self-interference cancellation in 5G and beyond," *IEEE Commun. Mag.*, vol. 52, no. 2, pp. 114–121, Feb. 2014.
[19] H. Kim, J. Kim, and D. Hong, "Dynamic TDD systems for 5G and beyond: A survey of cross-link interference mitigation," *IEEE Commun. Surveys Tuts.*, vol. 22, no. 4, pp. 2315–2348, 4th Quart., 2020.
[20] K. Pedersen, A. Esswie, D. Lei, J. Harrebek, Y. Yuk, S. Selvaganapathy, and H. Helmers, "Advancements in 5G new radio TDD cross link interference mitigation," *IEEE Wireless Commun.*, vol. 28, no. 4, pp. 106–112, Aug. 2021.
[21] *New SI: Study on Evolution of NR Duplex Operation*, document RP-213591, 2021. [Online]. Available: https://portal.3gpp.org/ngppapp/CreateTdoc.aspx?mode=view&contributionId=1284745
[22] *Study on Potential Enhancements on Dynamic/Flexible TDD*, document R1-2204531, 2022. [Online]. Available: https://portal.3gpp.org/ngppapp/CreateTdoc.aspx?mode=view&contributionId=1323361
[23] *Dynamic TDD Enhancements*, document R1-2204432, 2022. [Online]. Available: https://portal.3gpp.org/ngppapp/CreateTdoc.aspx?mode=view&contributionId=1323221
[24] *Study on New Radio Access Technology: Radio Frequency (RF) and Co-Existence Aspects*, document TR-38.803, 2017. [Online]. Available: https://portal.3gpp.org/desktopmodules/Specifications/SpecificationDetails.aspx?specificationId=3069
[25] *Realistic Power Amplifier Model for the New Radio Evaluation*, document R4-163314, 2016. [Online]. Available: https://portal.3gpp.org/ngppapp/CreateTdoc.aspx?mode=view&contributionId=703123
[26] *PA Model Using a Memory Polynomial*, document R4-167263, 2016. [Online]. Available: https://portal.3gpp.org/ngppapp/CreateTdoc.aspx?mode=view&contributionId=731291
[27] *Title 47 of the Code of Federal Regulations (CFR), Federal Communications Commission Std*, 2011.
[28] *Variation of the Boundary Between the Out-of-Band and Spurious Domains Required for the Application of Recommendations ITU-R SM.1541 and ITU-R SM.329*, document ITU-R SM.1539-1, 2002.
[29] *Unwanted Emissions in the Out-of-Band Domain Falling Into Adjacent Allocated Bands*, document ITU-R SM.1540, 2001.
[30] *Unwanted Emissions in the Out-of-Band Domain*, document ITU-R SM.1541-6, 2015.
[31] Z. Zhang, X. Chai, K. Long, A. V. Vasilakos, and L. Hanzo, "Full duplex techniques for 5G networks: Self-interference cancellation, protocol design, and relay selection," *IEEE Commun. Mag.*, vol. 53, no. 5, pp. 128–137, May 2015.
[32] P. V. Prasannakumar, M. A. Elmansouri, and D. S. Filipovic, "Wideband dual-polarized Bi-static simultaneous transmit and receive antenna system," in *Proc. IEEE Int. Symp. Antennas Propag. (APSURSI)*, Jun. 2016, pp. 1855–1856.
[33] C. Shi, W. Pan, and S. Shao, "RF wideband self-interference cancellation for full duplex phased array communication systems," in *Proc. IEEE Int. Conf. Commun. (ICC)*, May 2022, pp. 1094–1099.

XIANGHUI HAN received the M.S. degree in communication and information system from the Beijing University of Posts and Telecommunications, in 2015. He is currently pursuing the D.Eng. degree in electronic information with Southeast University. Since 2015, he has been with ZTE Corporation as a Standard Engineer. He actively participates in standardization work in 3GPP RAN1 Working Group, involving in 5G topics, such as ultra-reliable and low latency communications, coverage enhancement, sub-band full duplex operation and dynamic spectrum sharing. He is the RAN1 Feature Lead of several enhancements in Rel-17 and Rel-18.

RUIQI (RICHIE) LIU (Member, IEEE) received the B.S. and M.S. degrees (Hons.) in electronic engineering from the Department of Electronic Engineering, Tsinghua University, in 2016 and 2019, respectively. He is currently a Master Researcher with the Wireless Research Institute, ZTE Corporation, responsible for long-term research as well as standardization. He has served as the co-rapporteur of the work item (WI) on NR RRM enhancement and the feature lead of multiple features. He is the author or coauthor of several books and book chapters. During his three year service at 3GPP, from 2019 to 2022, he has authored and submitted more than 500 technical documents with over 100 of them approved. His research interests include reconfigurable intelligent surfaces, wireless positioning, quantum communication, and visible light communication. He is the Standardization Officer of IEEE ComSoc ETI on reconfigurable intelligent surfaces (ETI-RIS) and the Standards Liaison Officer of IEEE ComSoc Signal Processing and Computing for Communications Technical Committee (SPCC-TC). He received the Outstanding Service Award from the SPCC-TC, in 2022, and the Two Best Workshop Awards as the Chair. He has served as the Lead Guest Editor for the Special Issue on 6G in IEEE Open Journal of the Communications Society (OJCOMS). He is an Editor of *ITU Journal of Future and Evolving Technologies* (ITU J-FET) and an Associate Editor of *IET Quantum Communication*. He actively participates in organizing committees, technical sessions, workshops, symposia, and industry panels in IEEE conferences as the chair, an organizer, a moderator, and a panelist or an invited speaker. He currently serves as the Vice Chair for ISG RIS in ETSI.

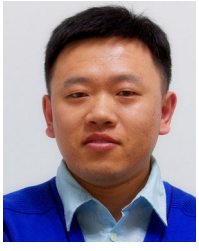

XING LIU received the M.S. degree from Harbin Engineering University (HEU), China, in 2010. He has been working as a Pre-Search Engineer with ZTE Corporation, since 2010. His research interests include sub-band full duplex operation, initial access, enhancement of ultra-reliable and low latency communications, multicast and broadcast services, and cognitive radio.

CHUNLI LIANG received the M.S. degree from Xiamen University (XMU), China, in 2005. She has been working as a Pre-Research Engineer with ZTE Corporation, since 2006. Her research interests include synchronization signal, physical uplink channel design, carrier aggregation, full duplex operation, enhancement of ultra-reliable and low latency, coverage enhancements, and multi-carrier operation.

XINGGUANG WEI received the M.S. degree from the Beijing University of Posts and Telecommunications (BUPT), China, in 2018. Since 2018, he has been working as a Standardization Engineer with ZTE Corporation. He has been involved in the 3GPP 5G standardization since the first NR release, i.e., Rel-15, mainly focusing on bandwith part, carrier aggregation, multicast/broadcast, and full duplex.

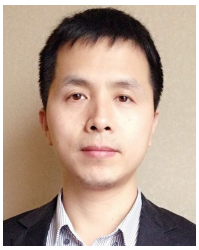

YUPENG HAO received the M.S. degree from the University of Chinese Academy of Sciences, China, in 2005. He is currently the Chief Engineer of wireless product planning with ZTE Corporation, leading the product planning for 4G/5G baseband technologies. His research interests include interference management, networking architecture, full duplex, and MIMO enhancement.

ZHAOTAO ZHANG received the M.S. degree from Southwest Jiaotong University, in 2005. He is currently pursuing the Ph.D. degree in electronic information with Southeast University. From 2005 to 2018, he was a Research and Development Engineer at ALU, Ericsson, Vodafone. Since 2018, he has been with Nanjing Research and Development Center of Broadband Wireless Communications as a Researcher. His research interests include distributive MIMO and 6G.

SHI JIN (Senior Member, IEEE) received the B.S. degree in communications engineering from the Guilin University of Electronic Technology, Guilin, China, in 1996, the M.S. degree from the Nanjing University of Posts and Telecommunications, Nanjing, China, in 2003, and the Ph.D. degree in information and communications engineering from Southeast University, Nanjing, in 2007. From June 2007 to October 2009, he was a Research Fellow at the Adastral Park Research Campus, University College London, London, U.K. He is currently a Faculty Member with the National Mobile Communications Research Laboratory, Southeast University. His research interests include space time wireless communications, random matrix theory, and information theory. He and his coauthors received the 2011 IEEE Communications Society Stephen O. Rice Prize Paper Award in the field of communication theory and the 2010 Young Author Best Paper Award from the IEEE Signal Processing Society. He serves as an Associate Editor for the IEEE TRANSACTIONS ON COMMUNICATIONS, IEEE TRANSACTIONS ON WIRELESS COMMUNICATIONS, IEEE COMMUNICATIONS LETTERS, and *IET Communications*.